Two-component Bose-Einstein condensates in periodic potential

N. A. Kostov,[1,*] V. Z. Enol'skii,[2,†] V. S. Gerdjikov,[2,‡] V. V. Konotop,[3,§] and M. Salerno[2,‖]
[1]*Institute for Electronics, Bulgarian Academy of Sciences, Boulevard Tzarigradsko chaussee 72, 1784 Sofia, Bulgaria*
[2]*Dipartimento di Fisica "E. R. Caianiello" and Istituto Nazionale di Fisica della Materia (INFM), Universitá di Salerno, via S. Allende, 184081 Baronissi (SA), Italy*
[3]*Centro de Física Teórica e Computacional and Departamento de Física, Universidade de Lisboa, Avenida Prof. Gama Pinto 2, Lisboa 1049-003, Portugal*
(Received 5 July 2003; revised manuscript received 4 June 2004; published 30 November 2004)

Coupled nonlinear Schrödinger (CNLS) equations with an external elliptic function potential model with high accuracy a quasi-one-dimensional interacting two-component Bose-Einstein condensate (BEC) trapped in a standing wave generated by a few laser beams. The construction of stationary solutions of the two-component CNLS equation with a periodic potential is detailed and their stability properties are studied by direct numerical simulations. Some of these solutions allow reduction to the Manakov system. From a physical point of view the trivial phase solutions can be interpreted as exact Bloch states at the edge of the Brillouin zone. Some of them are stable while others are found to be unstable against weak modulations of long wavelength. By numerical simulations it is shown that the modulationally unstable solutions lead to the formation of localized ground states of the coupled BEC system.

DOI: 10.1103/PhysRevE.70.056617 PACS number(s): 05.45.Yv, 42.65.−k, 03.75.Lm

I. INTRODUCTION

Recent experiments on dilute-gas Bose-Einstein condensates (BEC's) have generated great interest from both theoretical and experimental points of view [1]. At ultralow temperatures the mean-field description for the macroscopic BEC wave function is constructed using the Hartree-Fock approximation and results in the Gross-Pitaevskii (GP) equation [1]. The latter reduces to the one-dimensional (1D) nonlinear Schrödinger (NLS) equation with an external potential, in particular, when the transverse dimensions of the condensate are much less than its healing length and its longitudinal dimension is of the order of or much longer than the healing length (see, e.g., [2,3]). This is known as the *quasi-one-dimensional* (quasi-1D) regime of the GP equation. In this regime BEC's remain phase coherent, and the governing equations are one dimensional. Several families of stationary solutions for the cubic NLS equation with an elliptic function potential have been recently presented in Refs. [4,5] and their stability has been examined by analytic and numerical methods [5–7].

Experimental realization of two-component BEC's [8,9] has stimulated considerable attention in general [9] and in particular in the quasi-1D regime [10,11] when the GP equations for two interacting BEC's reduce to coupled nonlinear Schrödinger (CNLS) equations with an external potential. In specific cases the two-component CNLS equations can be reduced to the Manakov system [12] with an external potential.

An important role in analyzing these effects was played by the elliptic and periodic solutions of the above-mentioned equations. Such solutions for the one-component NLS equation are well known; see [13] and the numerous references therein. Elliptic solutions for the CNLS equation and Manakov system were derived in [14–16].

In the presence of an external elliptic potential explicit stationary solutions for the NLS equation were derived in [5–7]. These results were generalized to the *n*-component CNLS equation in [11].

We study exact stationary two-component solutions of the CNLS equation with elliptic external potential. Our main aim and interest will be on the physical implications of these solutions, in particular on the role played by unstable solutions in the generation of two-component solitons via the mechanism of modulational instability. Special attention will be devoted to a class of solutions with degenerate interaction matrices, as well as to the problem of the reduction of the original three-dimensional coupled GP equations to the coupled one-dimensional NLS equations. In particular, a criterion for the 1D approximation to be valid is derived. Possibilities of a physical realization of the considered situations are also briefly discussed.

The paper is organized as follows. In Sec. II we show how to derive 1D equations for coupled BEC's starting from the original three-dimensional problem using a multiple scale expansion in the small amplitude limit. In Sec. III we present an exact solution of the CNLS system with nontrivial phases. Section IV concerns stationary solutions with trivial phases for both proportional and nonproportional components. In Sec. V we discuss the physical properties of the trivial phase solutions and show, by means of direct numerical simulations, how these solutions may lead to the formation of localized matter waves through the mechanism of modula-

*Electronic address: nakostov@ie.bas.bg
†Electronic address: vze@ma.hw.ac.uk
‡Permanent address: Institute for Nuclear Research and Nuclear Energy, Bulgarian Academy of Sciences, Blvd. Tzarigradsko chaussee 72, 1784 Sofia, Bulgaria.
Electronic address: gerjikov@inrne.bas.bg
§Electronic address: konotop@cii.fc.ul.pt
‖Electronic address: salerno@sa.infn.it

tional instability. In Sec. VI we compare the present results with previous work and briefly discuss the possibility of experimental implementations. Finally, in Sec. VII we summarize the main conclusions of the paper.

II. BASIC EQUATIONS

At very low temperatures, when the mean-field approximation is applicable, the evolution of two interacting BEC's can be described by two coupled GP equations ($j=1, 2$) (see, e.g., [9,10])

$$i\hbar\frac{\partial\Psi_j}{\partial t}=\left[-\frac{\hbar^2}{2m}\nabla^2+V_j(\mathbf{r})+\frac{4\pi\hbar^2}{m}\sum_{l=1,2}a_{jl}|\Psi_l|^2\right]\Psi_j, \tag{2.1}$$

where the atomic masses of both components are assumed to be equal, $V_j(\mathbf{r})$ is an external trap potential, and a_{ij} are the scattering lengths of the respective atomic interactions (other notations are standard). In the case when the potential consists of a superposition of a magnetic trap providing a cigar-shaped condensate (elongated, say, along the x axis) and an optical lattice inducing a trap potential which is assumed to be periodic along the x axis, one has ($j=1, 2$)

$$V_j(\mathbf{r})=\frac{m}{2}\Omega_j^2(\lambda^2x^2+y^2+z^2)+U(\kappa x), \tag{2.2}$$

$$U(\kappa x)=U(\kappa(x+L)). \tag{2.3}$$

Here λ describes the aspect ratio of the condensate, which is assumed to be the same for both components. For the cigar-shaped condensates $\lambda\ll 1$ with typical values 10^{-2}–10^{-4}.

Although in the last expression we have imposed equality of the optical potential for both components, in a generic case one has to distinguish the linear oscillator frequencies Ω_1 and Ω_2 when considering the two components corresponding to the different magnetic moments. For example, in the experimental settings of [17] with ^{87}Rb atoms $\Omega=\Omega_2/\Omega_1=\sqrt{2}$. This fact has a natural implication for the resulting form of the effective system of coupled 1D NLS equations. Indeed, different oscillator frequencies mean that two components are located in two different parabolic potentials, and thus their effective densities are different when the number of atoms is equal. As a consequence, even at approximately equal s-wave scattering lengths, and thus for $a_{11}\approx a_{22}$, the two components will experience different nonlinearities, proportional to the atomic densities.

Another important issue to be mentioned here is that a cigar-shaped BEC can be viewed as a waveguide for matter waves. As such it is characterized by its mode structure. As is well known (compare with the nonlinear optical waveguides [18]) the intrinsic nonlinearity of a BEC results in mode interaction (and thus energy distribution among modes). If, however, the nonlinearity is weak enough, the main state of the condensate can be considered as a weakly modulated ground state, as it is clear that for a two-component BEC the corresponding small parameter is the ratio of the energy of two-body interactions $4\pi\hbar^2N_j\lambda^{1/2}a_{jj}/ma_j^3$ (here $a_j=\sqrt{\hbar/m\Omega_j}$ is the linear oscillator length and $N_j=\int|\Psi_j|^2d\mathbf{r}$ is the number of atoms of the jth component) to the kinetic energy $\hbar^2/2ma_j^2$. In other words, the small parameter of the problem can be identified formally as $\epsilon=8\pi N_1a_{11}\sqrt{\lambda}/a_1\ll 1$, where $N=N_1+N_2$ is the total number of atoms. Here we have taken into account that a_1 and a_2 as well as the scattering lengths between atoms a_{ij} are all of the same order. In this situation a self-consistent reduction of the original 3D system (2.1) to the effective 1D system of coupled equations can be provided by means of the multiple scale technique. Since the details of such a reduction have already been published elsewhere [3,19] for a single component BEC, here we only outline the main steps.

Let us first introduce dimensionless variables

$$\mathbf{r}'=(x',\mathbf{r}'_\perp)=\frac{\mathbf{r}}{a_1},\quad t'=\frac{1}{2}\Omega_1t,\quad \psi_j=\sqrt{\frac{2a_1^3}{N}}\Psi_j,$$

and rewrite Eqs. (2.1) in the form

$$i\dot{\psi}_1=[-\Delta'+U_1(\mathbf{r}'_\perp,x')+g_{11}|\psi_1|^2+g_{21}|\psi_2|^2]\psi_1, \tag{2.4}$$

$$i\dot{\psi}_2=[-\Delta'+U_2(\mathbf{r}'_\perp,x')+g_{12}|\psi_1|^2+g_{22}|\psi_2|^2]\psi_2, \tag{2.5}$$

where $\kappa'=\kappa a_1$,

$$U_1(\mathbf{r}'_\perp,x')=\lambda^2x'^2+\mathbf{r}'^2_\perp+V(\kappa'x'), \tag{2.6}$$

$$U_2(\mathbf{r}'_\perp,x')=\Omega^2(\lambda^2x'^2+\mathbf{r}'^2_\perp)+V(\kappa'x'),$$

$$\Omega=a_1^2/a_2^2,\quad V(\kappa'x')=\frac{2}{\hbar\Omega_1}U(\kappa'x'), \tag{2.7}$$

and $g_{ij}=4\pi Na_{ij}/a_1$. The next consideration depends on the magnitude of κ [it is assumed that $U'(x)/U(x)=O(1)$]. One can distinguish three main cases.

(i) $\kappa'\sim 1$. In this case the periodicity is of order of the transverse size of the condensate and much less than the healing length of each of the components, $\xi_j=(8\pi n_ja_j)^{-1/2}$, where n_j is the density of the jth component: $a_j^2/\xi_j^2\sim\epsilon$. Then, for excitations of the BEC having characteristic scales of order of the healing length, the periodicity modifies the spectrum of the underlying system, introducing the effective group velocity dispersion. The resulting equations are just CNLS equations without a periodic potential. This is the case similar to one considered in [3] for the case of a single-component BEC.

(ii) $\kappa'\ll\epsilon$ (say $\kappa\sim\epsilon^2$). In this case the periodic potential can be considered as smoothly varying on scales of order of the healing lengths, and somehow can be viewed as a limit of the case considered below.

(iii) $\kappa'=\alpha\epsilon$ where $\alpha\sim 1$. This is the case when the potential periodicity is of the order of the effective length of the nonlinearity (i.e., of the healing length). Below we concentrate on this last case.

To this end we consider two eigenvalue problems

$$(-\Delta'+\lambda^2x'^2+\mathbf{r}'^2_\perp)\varphi_1=E_1\varphi_1,$$

$$(-\Delta' + \Omega^2(\lambda^2 x'^2 + \mathbf{r}_\perp'^2))\varphi_2 = E_2\varphi_2 \tag{2.8}$$

whose normalized ground states are well known:

$$\varphi_1 = \frac{\lambda^{1/4}}{\pi^{3/4}} e^{-(\lambda x'^2 + \mathbf{r}_\perp'^2)/2},$$

$$\varphi_2 = \frac{\Omega^{3/4}\lambda^{1/4}}{\pi^{3/4}} e^{-(\Omega/2)(\lambda x'^2 + \mathbf{r}_\perp'^2)}, \tag{2.9}$$

and $E_j = \Omega^{j-1}(\lambda + 2)$.

The next steps are conventional for the multiple scale expansion (see, e.g., [3]); namely, we introduce scaled variables $x_n = \epsilon^n x'$, $\mathbf{r}_n = \epsilon^n \mathbf{r}_\perp'$, and $t_n = \epsilon^n t'$ ($n = 0, 1, 2, \ldots$) which are considered as independent, and look for the solution of Eqs. (2.4) and (2.5) in the form

$$\psi_j = \sqrt{\frac{1}{|g_{11}|\lambda^{1/2}}}\left(\epsilon\psi_j^{(1)} + \epsilon^2\psi_j^{(2)} + \cdots\right) \tag{2.10}$$

with

$$\psi_j^{(1)} = Q_j(x_1, t_2)\varphi_j(x_0, \mathbf{r}_0)e^{-iE_j t_0}, \quad j = 1, 2. \tag{2.11}$$

Here $Q_j(x_1, t_2)$ describes slow modulation of the background state (2.9) due to the nonlinearity.

Substituting Eq. (2.10) in Eqs. (2.4) and (2.5), equating all terms at each of the ϵ orders, and excluding secular terms, in the order ϵ^3 we obtain

$$i\frac{\partial Q_1}{\partial t_2} = -\frac{\partial^2 Q_1}{\partial x_1^2} + V(\alpha x_1)Q_1 + b_1|Q_1|^2 Q_1 + b_0|Q_2|^2 Q_1, \tag{2.12}$$

$$i\frac{\partial Q_2}{\partial t_2} = -\frac{\partial^2 Q_2}{\partial x_1^2} + V(\alpha x_1)Q_2 + b_0|Q_1|^2 Q_2 + b_2|Q_2|^2 Q_2, \tag{2.13}$$

where

$$b_1 = \mathrm{sgn}(g_{11})\int |\varphi_1|^4 d\mathbf{r} = \frac{\mathrm{sgn}(g_{11})}{2^{3/2}\pi^{3/2}},$$

$$b_0 = \frac{g_{12}}{|g_{11}|}\int |\varphi_1|^2|\varphi_2|^2 d\mathbf{r} = \frac{1}{\pi^{3/2}}\left(\frac{\Omega}{\Omega+1}\right)^{3/2}\frac{a_{12}}{|a_{11}|},$$

$$b_2 = \frac{g_{22}}{|g_{11}|}\int |\varphi_2|^4 d\mathbf{r} = \frac{\Omega^{3/2}}{2^{3/2}\pi^{3/2}}\frac{a_{22}}{|a_{11}|},$$

and it is taken into account that $a_{12} = a_{21}$. The system (2.12) and (2.13) is the subject of our main interest.

It is to be emphasized here that, although the trap potential is included in the evolution equations [see Eqs. (2.1) and (2.2)], it does not appear in an explicit form in the system (2.12) and (2.13) because $Q_{1,2}$ describe modulations of the ground state. The effect of the trap potential on the condensate dynamics is restored by reconstructing $\psi_j^{(1)}$ from the factorization (2.11). In the case when the healing length becomes comparable with the longitudinal size of the condensate the developed approach is not valid any more.

III. STATIONARY SOLUTIONS WITH NONTRIVIAL PHASES

An appropriate class of periodic potentials to model the quasi-1D confinement produced by a standing light wave is given by [5–7,11]

$$V(\alpha x) = V_0 \mathrm{sn}^2(\alpha x, k), \tag{3.1}$$

where $\mathrm{sn}(\alpha x, k)$ denotes the Jacobian elliptic sine function with elliptic modulus $0 \leqslant k \leqslant 1$. In experiments such potentials can be well approximated by only a few laser beams. Indeed, one can use the well known formula [20]

$$\mathrm{sn}(\alpha x; k) = \frac{2\pi}{kK(k^2)}\sum_{n=0}^{\infty}\frac{q^{n+1/2}}{1-q^{2n+1}}\sin\frac{(2n+1)\pi\alpha x}{2K(k^2)}$$

where $q = \exp\{-\pi[K(1-k^2)/K(k^2)]\}$ and $K(k^2)$ is a complete elliptic integral of the first kind. Then, even for relatively large elliptic modulus, say $k_0^2 = 0.9$, one obtains $q \approx 0.084$ which means that potentials of the form

$$V(\alpha x) = \frac{2V_0\pi^2 q}{k^2K^2(k^2)(1-q)^2}\left[1 - \cos\frac{\pi\alpha x}{K(k^2)} + \frac{2q}{1+q+q^2}\left(\cos\frac{\pi\alpha x}{K(k^2)} - \cos\frac{2\pi\alpha x}{K(k^2)}\right)\right],$$

with $k < k_0$, which can be produced by using only two laser beams, are approximated by Eq. (3.1) with accuracy higher than 99%. The accuracy of the approximation increases as k decreases, and thus Eq. (3.1) appears to be a good approximation for experimentally producible potentials for a rather wide range of parameters.

After the change of notation $t_2 \to t, x_1 \to x$, the system (2.12), (2.13) takes the well known form

$$i\frac{\partial Q_1}{\partial t} + \frac{\partial^2 Q_1}{\partial x^2} - (b_1|Q_1|^2 + b_0|Q_2|^2)Q_1 - V_0\mathrm{sn}^2(\alpha x, k)Q_1 = 0, \tag{3.2}$$

$$i\frac{\partial Q_2}{\partial t} + \frac{\partial^2 Q_2}{\partial x^2} - (b_0|Q_1|^2 + b_2|Q_2|^2)Q_2 - V_0\mathrm{sn}^2(\alpha x, k)Q_2 = 0. \tag{3.3}$$

We restrict our attention to stationary solutions of CNLS equations of the type (see also [11])

$$Q_j(x,t) = q_j(x)\exp[-i\omega_j t + i\Theta_j(x) + i\kappa_{0,j}], \tag{3.4}$$

where $j = 1, 2$, $\kappa_{0,j}$ are constant phases, and q_j and $\Theta_j(x)$ are real-valued functions connected by the relation

$$\Theta_j(x) = \mathcal{C}_j\int_0^x \frac{dx'}{q_j^2(x')}, \tag{3.5}$$

$\mathcal{C}_j, j = 1, 2$, being constants of integration.

Following [5] we refer to solutions in the cases $\mathcal{C}_j = 0$ and $\mathcal{C}_j \neq 0$ as trivial and nontrivial phase solutions, respectively. We notice that nontrivial phase solutions imply nonzero current of the matter—it is proportional to $|q_j(x)|^2 d\Theta_j/dx = \mathcal{C}_j$, for each of the components—along the x axis, and hence

may have no direct relation to the experimental setting where BEC's are confined to a parabolic trap, while it could be relevant to BEC's having toroidal configurations. Also a system of coupled NLS equations appears to be a general model, having, for example, applications in nonlinear optics (see, e.g., [18]). Bearing this in mind we consider both types of solutions.

Substituting the ansatz (3.4) in Eqs. (2.12), (2.13) and separating the real and imaginary part we get

$$q_1^3 q_{1xx} - (b_1 q_1^2 + b_0 q_2^2) q_1^4 - V_0 \mathrm{sn}^2(\alpha x,k) q_1^4 + \omega_1 q_1^4 = \mathcal{C}_1^2, \tag{3.6}$$

$$q_2^3 q_{2xx} - (b_0 q_1^2 + b_2 q_2^2) q_2^4 - V_0 \mathrm{sn}^2(\alpha x,k) q_2^4 + \omega_2 q_2^4 = \mathcal{C}_2^2. \tag{3.7}$$

We analyze the solutions of type A in the terminology of [11] for $q_j^2, j=1, 2$, as a quadratic function of $\mathrm{sn}(\alpha x,k)$:

$$q_j^2 = A_j \mathrm{sn}^2(\alpha x,k) + B_j. \tag{3.8}$$

Inserting Eq. (3.8) in Eqs. (3.6), (3.7) and equating the coefficients of equal powers of $\mathrm{sn}(\alpha x,k)$ results in the following relations among the solution parameters $\omega_j, \mathcal{C}_j, A_j$, and B_j and the characteristic of the optical lattice V_0, α, and k:

$$A_1 = \frac{(b_0 - b_2)W}{\Delta}, \quad A_2 = \frac{(b_0 - b_1)W}{\Delta}, \tag{3.9}$$

$$B_j = -\beta_j A_j, \quad \mathcal{C}_j^2 = \alpha^2 A_j^2 \beta_j (\beta_j - 1)(1 - \beta_j k^2), \tag{3.10}$$

$$\omega_j = (1 + k^2)\alpha^2 + \frac{W}{\Delta}[\beta_1 b_1 (b_2 - b_0) - \beta_2 b_0 (b_0 - b_1)] - k^2 \alpha^2 \beta_j, \tag{3.11}$$

where $j=1, 2$ and

$$W = V_0 - 2\alpha^2 k^2, \quad \Delta = b_1 b_2 - b_0^2. \tag{3.12}$$

The results (3.8)–(3.11) will be consistent with the parametrization (3.4) and (3.5) if we ensure that both $q_j(x)$ and $\Theta_j(x)$ are real valued; this means that $\mathcal{C}_j^2 \geqslant 0$ and $q_j^2(x) \geqslant 0$. An elementary analysis shows that this is true provided one of the following pairs of conditions is satisfied ($j=1, 2$):

$$\text{(a)} \quad A_j \geqslant 0, \quad \beta_j \leqslant 0, \tag{3.13}$$

$$\text{(b)} \quad A_j \leqslant 0, \quad 1 \leqslant \beta_j \leqslant \frac{1}{k^2}. \tag{3.14}$$

The solutions Q_j in Eq. (3.4) are *not* necessarily periodic in x; periodicity will be present provided $q_j(x)$ and $\Theta_j(x)$ have commensurable periods. This holds true only under certain conditions on the solution parameters. Indeed, let us first calculate explicitly $\Theta_j(x)$ by using the well known formula (see, e.g., [20]):

$$\int_0^x \frac{du}{\wp(\alpha u) - \wp(\alpha v)} = \frac{1}{\wp'(\alpha v)}\left[2x\zeta(\alpha v) + \frac{1}{\alpha}\ln\frac{\sigma(\alpha x - \alpha v)}{\sigma(\alpha x + \alpha v)}\right].$$

Please use standard Weierstrass $\wp$ function.

In the case (a) we replace v by iv_j, set

$$\mathrm{sn}^2(i\alpha v_j;k) = \beta_j < 0, \quad e_1 = \frac{1}{3}(2 - k^2),$$

$$e_2 = \frac{1}{3}(2k^2 - 1), \quad e_3 = -\frac{1}{3}(1 + k^2), \tag{3.15}$$

and rewrite the left-hand side in terms of Jacobi elliptic functions:

$$\mathrm{sn}^2(i\alpha v;k)\int_0^x \frac{du\ \mathrm{sn}^2(\alpha u;k)}{\mathrm{sn}^2(i\alpha v;k) - \mathrm{sn}^2(\alpha u;k)} = -\beta_j x - \beta_j^2 \int_0^x \frac{du}{\mathrm{sn}^2(\alpha u,k) - \beta_j}.$$

Skipping the details we find the explicit form of $\Theta_j(x)$:

$$\Theta_j(x) = \mathcal{C}_j \int_0^x \frac{du}{A_j[\mathrm{sn}^2(\alpha u;k) - \beta_j]} = -\tau_j x + \frac{i}{2}\ln\frac{\sigma(\alpha x + i\alpha v_j)}{\sigma(\alpha x - i\alpha v_j)},$$

$$\tau_j = i\alpha\zeta(i\alpha v_j) + \frac{\alpha}{\beta_j}\sqrt{-\beta_j(1 - \beta_j)(1 - k^2\beta_j)}. \tag{3.16}$$

These formulas provide an explicit expression for the solutions $Q_j(x,t)$ with nontrivial phases; note that for real values of $v_j, \Theta_j(x)$ are also real.

Now we can find the conditions under which $Q_j(x,t)$ are periodic. Indeed, from Eq. (3.16) we can calculate the quantities T_j satisfying

$$\Theta_j(x + T_j) - \Theta_j(x) = 2\pi p_j, \tag{3.17}$$

with $p_j$integers. If the parameters β_j and v_j, related to β_j via (3.15), are such that the quantities

$$-\pi[\alpha v_j \zeta(\omega) + \omega\tau_j/\alpha]^{-1} = \frac{m_j}{p_j}, \quad j = 1,2, \tag{3.18}$$

are rational numbers (i.e., m_j and p_j are integers), then $Q_1(x)$ and $Q_2(x)$ are periodic with periods T_1 and T_2, respectively. We recall that ω (and ω') are the half periods of the Weierstrass functions. One can also find the smallest common period of $Q_1(x)$ and $Q_2(x)$.

Of course the trivial phase solutions considered in the next sections are always periodic functions of x.

We will list also solutions for two particular choices of b_1, b_2, and b_0 which can be viewed as singular limits of the generic case considered above. The first one is

$$b_0^2 = b_1 b_2, \quad b_1 \neq b_2, \tag{3.19}$$

which corresponds to the case (3.13). Then the solution is given by

$$A_2 = -\frac{b_1}{b_0}A_1, \quad V_0 = 2k^2\alpha^2,$$

$$\omega_1 = (\beta_2 - \beta_1)b_1 A_1 + (1 + k^2)\alpha^2 - \alpha^2 k^2 \beta_1,$$

$$\omega_2 = (\beta_1 - \beta_2)b_1 A_1 + (1 + k^2)\alpha^2 - \alpha^2 k^2 \beta_2,$$

TABLE I. Trivial phase solutions in the generic case $\Delta \equiv b_1 b_2 - b_0^2 \neq 0$. The conditions $c_k, k=1,\ldots,4$, are listed in Eq. (4.5).

Case 1	$q_1=\gamma_1 \mathrm{sn}(\alpha x,k)$	$\omega_1=-b_0 Y_1 W+\alpha^2(k^2+1)$	$\gamma_1^2=Y_2 W$	c_1
	$q_2=\gamma_2 \mathrm{cn}(\alpha x,k)$	$\omega_2=-b_2 Y_1 W+\alpha^2$	$\gamma_2^2=-Y_1 W$	
Case 2	$q_1=\gamma_1 \mathrm{dn}(\alpha x,k)$	$\omega_1=-b_1 Y_2 W/k^2+\alpha^2 k^2$	$\gamma_1^2=-Y_2 W/k^2$	c_2
	$q_2=\gamma_2 \mathrm{sn}(\alpha x,k)$	$\omega_2=-b_0 Y_2 W/k^2+\alpha^2(k^2+1)$	$\gamma_2^2=Y_1 W$	
Case 3	$q_1=\gamma_1 \mathrm{dn}(\alpha x,k)$	$\omega_1=-(b_0 Y_1+b_1 Y_2/k^2)W+\alpha^2 k^2$	$\gamma_1^2=-Y_2 W/k^2$	c_3
	$q_2=\gamma_2 \mathrm{cn}(\alpha x,k)$	$\omega_2=-(b_2 Y_1+b_0 Y_2/k^2)W+\alpha^2$	$\gamma_2^2=-Y_1 W$	
Case 4	$q_1=\gamma_1 \mathrm{sn}(\alpha x,k)$	$\omega_1=\omega_2=\alpha^2(k^2+1)$	$\gamma_1^2=Y_2 W$	c_4
	$q_2=\gamma_2 \mathrm{sn}(\alpha x,k)$		$\gamma_2^2=Y_1 W$	
Case 5	$q_1=\gamma_1 \mathrm{cn}(\alpha x,k)$	$\omega_1=\omega_2=\alpha^2+W$	$\gamma_1^2=-Y_2 W$	c_3
	$q_2=\gamma_2 \mathrm{cn}(\alpha x,k)$		$\gamma_2^2=-Y_1 W$	
Case 6	$q_1=\gamma_1 \mathrm{dn}(\alpha x,k)$	$\omega_1=\omega_2=\alpha^2 k^2+W/k^2$	$\gamma_1^2=-Y_2 W/k^2$	c_3
	$q_2=\gamma_2 \mathrm{dn}(\alpha x,k)$		$\gamma_2^2=-Y_1 W/k^2$	

$$\mathcal{C}_j^2 = \alpha^2 A_j^2 \beta_j(\beta_j - 1)(1 - \beta_j k^2),$$

$$B_j = -\beta_j A_j, \quad j = 1,2. \tag{3.20}$$

The second particular case is the Manakov system; it corresponds to the choice $b_1=b_2=b$. The result is

$$\omega_j = -b(\beta_1 A_1 + \beta_2 A_2) + (1+k^2)\alpha^2 - \alpha^2 k^2 \beta_j,$$

$$\mathcal{C}_j^2 = \alpha^2 A_j^2 \beta_j(\beta_j - 1)(1 - \beta_j k^2),$$

$$B_j = -\beta_j A_j, \quad V_0 = -b(A_1 + A_2) + 2k^2\alpha^2, \tag{3.21}$$

$j=1$, 2. In the two-component CNLS equations (3.6) and (3.7) the constants b_1, b_2, and b_0 are assumed to be negative. However, we have not used this restriction and our formulas are valid also for positive values of b_1, b_2, and b_0. It is possible to analyze also nontrivial phase solutions in the trigonometric $k \to 0$ and hyperbolic $k \to 1$ limits, which we will omit.

IV. TRIVIAL PHASE SOLUTIONS

In this section we consider solutions of (3.2) and (3.3) with trivial phase, i.e., $\mathcal{C}_1=\mathcal{C}_2=0$,

$$Q_j(x,t) = e^{-i\omega_j t + i\kappa_{0,j}} q_j(x), \quad j = 1,2, \tag{4.1}$$

and we will look for different possible choices for the functions $q_1(x)$ and $q_2(x)$. This type of solution is more flexible and in certain cases survives reductions of the constants $b_0^2 = b_1 b_2$ or the limit to the Manakov case: $b_1=b_2=b_0$. The solutions are also relevant for processes in BEC's and nonlinear optics [18].

In the following we shall consider the $q_i(x)$ to be expressed in terms of Jacobi elliptic functions, i.e., we assume the following ansatz: $q_j(x)=\gamma_j J_j(x)$, with $J_j(x), j=1$, 2, being one of the Jacobi elliptic function $\mathrm{sn}(\alpha x,k), \mathrm{cn}(\alpha x,k)$, or $\mathrm{dn}(\alpha x,k)$ and γ_i specifying the real amplitudes in Eq. (4.1). Note that the CNLS equations (3.2) and (3.3) possess the gauge invariance $Q_j \to Q_j e^{-i\kappa_{0,j}}$. This allows one to fix up conveniently the initial phases of both $Q_j(x)$. In most of the following examples we have made this choice by requiring that $\gamma_j^2 > 0$. Direct substitution of the above ansatz into Eqs. (3.2) and (3.3) provides a set of algebraic equations for the parameters whose solutions furnish exact ground states of the coupled BEC system.

For completeness, we shall briefly illustrate the calculations for case 1 in Table I (see also [11]) for which

$$q_1(x) = \gamma_1 \mathrm{sn}(\alpha x,k), \quad q_2(x) = \gamma_2 \mathrm{cn}(\alpha x,k). \tag{4.2}$$

The functions in Eq. (4.1) are solutions of Eq. (3.2) provided the constants satisfy the relations

$$b_0\gamma_2^2 - b_1\gamma_1^2 - W = 0,$$

$$b_2\gamma_2^2 - b_0\gamma_1^2 - W = 0,$$

$$\omega_1 - \alpha^2(k^2+1) - b_0\gamma_2^2 = 0,$$

$$\omega_2 - \alpha^2 - b_2\gamma_2^2 = 0, \tag{4.3}$$

where W is defined in Eq. (3.12). From this system we can determine four of the constants in terms of the others. Let us split them into two groups. The first one,

$$G_1 \simeq \{b_1, b_2, b_0, W, \alpha, k\},$$

consists of constants determining the equations and the potential and we assume they are fixed. The second group of constants

$$G_2 \simeq \{\omega_1, \omega_2, \gamma_1, \gamma_2\}$$

characterizes the corresponding soliton solution. Next we solve Eq. (4.3) and express the constants G_2 in terms of G_1.

We have collected all the results for generic choices of b_0, b_1, and b_2 in Table I using the following notation:

$$Y_1 = \frac{b_1 - b_0}{b_0^2 - b_1 b_2}, \quad Y_2 = \frac{b_2 - b_0}{b_0^2 - b_1 b_2}, \tag{4.4}$$

and the conditions

TABLE II. Trivial phase solutions in the case $\Delta \equiv b_1 b_2 - b_0^2 = 0$.

Case 1	$q_1 = \gamma_1 \mathrm{sn}(\alpha x, k)$	$\omega_1 = \alpha^2(k^2+1) + b_1\gamma_1^2$	$\gamma_2^2 = \sqrt{b_1/b_2}\,\gamma_1^2$	$W=0$
	$q_2 = \gamma_2 \mathrm{cn}(\alpha x, k)$	$\omega_2 = \alpha^2 + b_0\gamma_1^2$		
Case 2	$q_1 = \gamma_1 \mathrm{dn}(\alpha x, k)$	$\omega_1 = \alpha^2 k^2 + b_1\gamma_1^2$	$\gamma_2^2 = k^2\sqrt{b_1/b_2}\,\gamma_1^2$	$W=0$
	$q_2 = \gamma_2 \mathrm{sn}(\alpha x, k)$	$\omega_2 = \alpha^2(k^2+1) + b_0\gamma_1^2$		

$$c_1 = \begin{cases} W>0, & Y_2>0, \quad Y_1<0 \quad \text{or} \\ W<0, & Y_2<0, \quad Y_1>0 \end{cases}$$

$$c_2 = \begin{cases} W>0, & Y_2<0, \quad Y_1>0 \quad \text{or} \\ W<0, & Y_2>0, \quad Y_1<0 \end{cases}$$

$$c_3 = \begin{cases} W>0, & Y_2<0, \quad Y_1<0 \quad \text{or} \\ W<0, & Y_2>0, \quad Y_1>0 \end{cases}$$

$$c_4 = \begin{cases} W>0, & Y_2>0, \quad Y_1>0 \quad \text{or} \\ W<0, & Y_2<0, \quad Y_1<0 \end{cases} \tag{4.5}$$

which ensure that $\gamma_1^2>0$ and $\gamma_2^2>0$.

In Tables II and III we treat special situations: (i) $b_0^2 = b_1 b_2$ (Table II) and (ii) $b_1 = b_2 = b$ (Table III), where $X = -W/(b_0+b)$. The transition from the generic case to (i) is singular. The Manakov case is obtained for $b_0 = b_1 = b_2 = b$ and follows easily from the results in Table III.

The solutions in cases 1 and 2 exclude the possibility to have $b_1 = b_2$ and $\gamma_j^2 > 0$. One can check that for $b_1 = b_2$ we have $\gamma_1^2 + \gamma_2^2 = 0$ for case 1 and $\gamma_1^2 + k^2\gamma_2^2 = 0$ in case 2. In all these cases either γ_1^2 or γ_2^2 must be negative.

In the last three cases the two components are proportional: $q_1(x) = \gamma q_2(x)$ and $q_1(x)$ is one of the three functions $\mathrm{sn}(\alpha x, k), \mathrm{cn}(\alpha x, k)$, or $\mathrm{dn}(\alpha x, k)$. Such an ansatz imposes on the system (3.2) and (3.3) the compatibility condition

$$\gamma^2(b_2 - b_0) + b_0 - b_1 = 0, \tag{4.6}$$

which is equivalent to $b_1 = b_2$. If Eq. (4.6) is satisfied the system (3.2) and (3.3) reduces effectively to the one-component case, which has already been studied; see [5–7] and the discussion in Sec. VI below.

V. MODULATIONAL INSTABILITY OF THE TRIVIAL PHASE SOLUTIONS AND LOCALIZED MATTER WAVE GENERATION

In this section we discuss the stability of the above solutions from a physical point of view. To this end we remark that all the trivial phase solutions are periodic functions of period twice the period of the lattice [recall that the period a of the potential in Eq. (3.1) is $a = 2K(k^2)/\alpha$, where $K(k^2)$ is the complete elliptic integral of the first kind]. The corresponding wave number of these solutions is $\mathcal{K} = \pi/a$ which is just the boundary of the Brillouin zone of the uncoupled periodic linear system.

Moreover, one can easily check that each component $q_i(x), i = 1, 2$, satisfies the Bloch condition

$$q_j(x + R_n) = e^{i\mathcal{K}R_n} q_j(x), \quad R_n = na, \quad n \in N, \tag{5.1}$$

i.e., the trivial phase solutions are exact *nonlinear* Bloch states [a nonlinear Bloch state can be defined, in analogy with the linear case, as a state for which Eq. (5.1) is satisfied]. Although nonlinearity does not compromise the Bloch property (this being a direct consequence of the translation invariance of the lattice), it can drastically influence the stability of the states through a modulational instability mechanism.

The possibility that localized states of soliton type can be generated from modulational instability of Bloch states at the edge of the Brillouin zone was observed, both analytically and numerically, for a single component BEC in an optical lattice in the cases of one [3], two, and three spatial dimensions [19]. In order to explore the same possibility of this occurring also in the present periodic two-component system we have recourse to numerical simulations. To this end we have integrated Eqs. (3.2) and (3.3) with an operator splitting method using fast Fourier transform, taking as initial conditions the exact solutions derived above modulated by a long

TABLE III. Trivial phase solutions in the case $b_1 = b_2 = b$.

Case 3	$q_1 = \gamma_1 \mathrm{dn}(\alpha x, k)$	$\omega_1 = \alpha^2 k^2 - (b_0 + b/k^2)X$	$\gamma_1^2 = -X/k^2$	$W<0$
	$q_2 = \gamma_2 \mathrm{cn}(\alpha x, k)$	$\omega_2 = \alpha^2 - (b + b_0/k^2)X$	$\gamma_2^2 = -X$	
Case 4	$q_1 = \gamma_1 \mathrm{sn}(\alpha x, k)$	$\omega_1 = \omega_2 = \alpha^2(k^2+1)$	$\gamma_1^2 = \gamma_2^2 = X$	$W>0$
	$q_2 = \gamma_2 \mathrm{sn}(\alpha x, k)$			
Case 5	$q_1 = \gamma_1 \mathrm{cn}(\alpha x, k)$	$\omega_1 = \omega_2 = \alpha^2 + W$	$\gamma_1^2 = \gamma_2^2 = -X$	$W<0$
	$q_2 = \gamma_2 \mathrm{cn}(\alpha x, k)$			
Case 6	$q_1 = \gamma_1 \mathrm{dn}(\alpha x, k)$	$\omega_1 = \omega_2 = \alpha^2 k^2 + W/k^2$	$\gamma_1^2 = \gamma_2^2 = -X/k^2$	$W<0$
	$q_2 = \gamma_2 \mathrm{dn}(\alpha x, k)$			

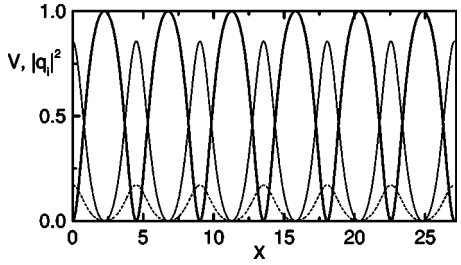

FIG. 1. Initial profile of a stable cn-cn solution plotted against the potential profile (thick curve). The dashed and solid thin curves denote the modulus squared of q_1 and q_2, respectively. The parameters are fixed as $k^2=0.8, V_0=1, \alpha=1, b_0=-0.5, b_1=-1.0, b_2=-0.6$. The initial amplitudes are $\gamma_1=0.414\,039$, $\gamma_2=0.925\,82$.

wavelength $L(2\pi/k \ll \pi/L)$ and small amplitude sinusoidal profile.

In Fig. 1 we depict the initial profiles of the two-component cn-cn solution plotted against the potential profile, while in Fig. 2 we show the time evolution of this solution in the presence of a small modulation.

From Fig. 1 we see that the profiles remain stable for a long time for both components, indicating that the cn-cn solution is stable against small modulations. The main characteristic features of the modulational instability in the case of small amplitudes can be understood within the framework of the approach developed in [3,19]. In this regard, we assume that the perturbations of the nonlinear Bloch states have wavelength much larger than the period of the potential in Eqs. (3.2) and (3.3). Then, by analogy with Sec. II, one can look for solutions Q_j in the form $Q_j=\phi_j(x_0)\tilde{Q}_j(x_1,t_1)$, where $\phi_j(x_0)$ denote two chosen Bloch functions $\phi_{n,\kappa}(x_0)$ of the potential $V(\alpha x)$,

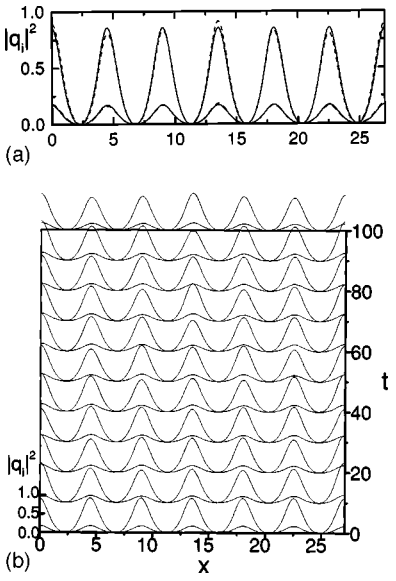

FIG. 2. Prospective view of the time evolution of the two-component cn-cn solution reported in Fig. 1. To check stability the solution was slightly modulated in space with a profile of the form $0.1\cos(0.2x)$. The top compares the profiles of the modulated (dashed line) and exact (continuous line) two component solution at time $t=100$. Parameters are fixed as in Fig. 1.

$$-\frac{d^2\phi_{n,\kappa}(x)}{dx^2}+V(\alpha x)\phi_{n,\kappa}(x)=\mathcal{E}_n(\kappa)\phi_{n,\kappa}(x), \qquad (5.2)$$

with n and κ denoting the number of the zone and the wave vector reduced to the first Brillouin zone, respectively (notice that we adopt again scaled variables). The Bloch functions are chosen to be normalized as follows: $\int_0^a|\phi_j(x)|^2dx=1$. One can then use these Bloch states as the zero order in a multiple scale expansion, in analogy to what was done in Sec. II and in Ref. [3]. Here we shall drop the details and present just the final system of equations for the amplitudes of the modulation field:

$$i\frac{\partial\tilde{Q}_1}{\partial t}+\frac{1}{2M_1}\frac{\partial^2\tilde{Q}_1}{\partial x^2}-(\tilde{b}_1|\tilde{Q}_1|^2+\tilde{b}_0|\tilde{Q}_2|^2)\tilde{Q}_1=0, \qquad (5.3)$$

$$i\frac{\partial\tilde{Q}_2}{\partial t}+\frac{1}{2M_2}\frac{\partial^2\tilde{Q}_2}{\partial x^2}-(\tilde{b}_0|\tilde{Q}_1|^2+\tilde{b}_2|\tilde{Q}_2|^2)\tilde{Q}_2=0, \qquad (5.4)$$

where we have introduced the following notation:

$$\frac{1}{M_j}=\frac{d^2\mathcal{E}_j(\kappa)}{d\kappa^2},$$

$$\tilde{b}_{1,2}=b_{1,2}\int_0^a|\phi_{1,2}(x)|^4dx,$$

$$\tilde{b}_0=b_0\int_0^a|\phi_1(x)|^2|\phi_2(x)|^2dx.$$

In Fig. 3 we depict the first two bands and the corresponding reciprocal effective masses of the underlying linear system in Eq. (5.2). To study modulational instability, we look for a solution of Eqs. (5.3) and (5.4) in the form of a weakly modulated constant background

$$\tilde{Q}_j=(\tilde{\gamma}_j+\tilde{\alpha}_je^{iKx-i\Omega t}+\tilde{\beta}_je^{-iKx+i\Omega t})e^{-i\nu_j t},$$

where $\nu_1=-\tilde{b}_1\tilde{\gamma}_1^2-\tilde{b}_0\tilde{\gamma}_2^2, \nu_2=-\tilde{b}_2\tilde{\gamma}_2^2-\tilde{b}_0\tilde{\gamma}_1^2$, and $|\tilde{\alpha}_j|,|\tilde{\beta}_j| \ll|\tilde{\gamma}_j|^2$. Next, we linearize the system with respect to $\tilde{\alpha}_j,\tilde{\beta}_j$ and derive the dispersion relation of the resulting linear system in the form

$$\Lambda^2-(G_1^2+G_2^2-2\tilde{\chi}_1G_1-2\tilde{\chi}_2G_2)\Lambda+G_1G_2[(G_1+2\tilde{\chi}_1)\times(G_2+2\tilde{\chi}_2)-4\tilde{\chi}_0^2]=0, \qquad (5.5)$$

where $\Lambda=\Omega^2, G_j=K^2/(2M_j), \tilde{\chi}_j=-\tilde{\gamma}_j^2\tilde{b}_j$ for $j=1$, 2, and $\tilde{\chi}_0=-\tilde{\gamma}_1\tilde{\gamma}_2\tilde{b}_0$. The corresponding solution of the coupled nonlinear system (consisting of two nonlinear Bloch waves) is stable if both roots of Eq. (5.5) are positive and unstable otherwise (notice that this analysis gives stability with respect to long wavelengths only).

As a particular example we shall consider the case in which both components belong to the same gap edge, i.e., when $M_1M_2>0$ and therefore $G_1G_2>0$. For the stability of the wave, then, the following conditions must be satisfied:

$$G_1^2+G_2^2-2\tilde{\chi}_1G_1-2\tilde{\chi}_2G_2>0, \qquad (5.6)$$

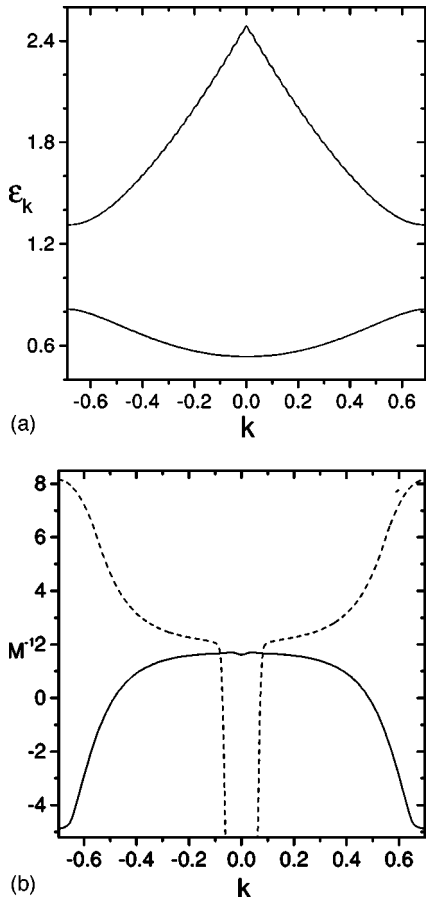

FIG. 3. (a) Lowest two bands of the linear Schrödinger problem in Eq. (5.2) in the reduced zone scheme. (b) Reciprocal effective masses of the first (continuous curve) and second (dashed curve) bands of (a). The parameter values of the potential are fixed as in Fig. 1. For these parameters the period of the potential is 4.5144 and the edges of the Brillouin zone are ±0.696.

$$G_1G_2 + 2(\tilde{\chi}_1G_2 + \tilde{\chi}_2G_1) > 4\tilde{\chi}_0^2 - 4\tilde{\chi}_1\tilde{\chi}_2. \tag{5.7}$$

Since the cases that we are studying numerically and are of physical interest correspond to negative b_j and $b_1b_2 > b_0^2$, we have that $\tilde{\chi}_j > 0$ and $\tilde{\chi}_1\tilde{\chi}_2 > \tilde{\chi}_0^2$. This implies that either (5.6) or (5.7) is satisfied for all K if either $M_{1,2} < 0$ or $M_{1,2} > 0$. In the case $M_{1,2} < 0$ the condition (5.7) can be viewed as a constraint on the wave amplitude. Indeed, after some algebra, one gets that (5.7) holds for any K if the following equation is satisfied:

$$(M_1\tilde{\chi}_1 + M_2\tilde{\chi}_2)^2 < 4M_1M_2(\tilde{\chi}_1\tilde{\chi}_2 - \tilde{\chi}_0^2). \tag{5.8}$$

In the second case, i.e., when $M_{1,2} > 0$, each of the states is unstable with respect to large wavelength excitations.

Now we can give a qualitative physical interpretation of the result depicted in Figs. 1 and 2. As follows from the explicit form of the solution, both components are described by the states belonging to the same edge of the Brillouin zone. This also can be viewed by the fact that $\nu_1 = \nu_2 \approx 0.6$ and thus the frequency of the solution is $\omega + \nu_{1,2} \approx 1$. Then, from Fig. 3(a) one concludes that both waves correspond to the states at the edge of the Brillouin zone and border the gap from the side of negative effective masses (this also follows from the fact that the period of the waves is twice the period of the potential and thus BEC's in the neighbor potential wells have opposite phases). Thus Eq. (5.6) is satisfied.

Next, we consider Eq. (5.8) whose left- and right-hand sides in the present case can be estimated as $[|M_1| = |M_2| \approx 0.238$; see Fig. 3(b)] 0.0266 and 0.352, respectively. Thus the stability of the solution observed in numerical simulations is confirmed by our stability analysis.

Let us now consider the case in which two atomic components belong to different edges of the gap, so that $M_1 > 0$ and $M_2 < 0$ (and hence $G_1 > 0$ and $G_2 < 0$) and restrict the consideration to the case of positive b_j. Then for the stability of the wave, the following conditions must be satisfied:

$$2\tilde{\chi}_1G_1 < G_1^2 + G_2^2 + 2\tilde{\chi}_2|G_2|, \tag{5.9}$$

$$2\tilde{\chi}_2G_1 < G_1|G_2| + 2\tilde{\chi}_1|G_2|. \tag{5.10}$$

In this case the first component, having positive effective mass, has a self-attractive character, which might dominate the destructive action of the lattice when the matter localizes around the potential maxima. In the absence of the second component, this wave would be modulationally unstable, this being a well known fact which can be seen also from Eq. (5.9) (take $\tilde{\chi}_0$ and G_2 to be equal to zero). On the other hand, the second component, with negative effective mass, has a self-repulsive character, which is compensated by the potential barriers provided its localization occurs around the minima of the lattice potential. This component is stable even in the absence of the first harmonic and if its amplitude is large enough (or the amplitude of the first component is small enough) it can help to stabilize the first component, as follows from Eq. (5.9). More specifically Eq. (5.9) is satisfied for any K if

$$\tilde{\gamma}_1^2 < \frac{\tilde{b}_2M_1}{\tilde{b}_1|M_2|}\tilde{\gamma}_2^2. \tag{5.11}$$

The above analysis is in good qualitative agreement with the results of numerical experiments. In particular, we find that except for the cn-cn solution all other solutions display modulational instability which leads to the formation of localized states. This is clearly seen in Fig. 4 where the time evolution of the unstable sn-sn solution is reported (notice the formation of two localized excitations at time $t = 40$). As for the previous case, the instability of this solution can be easily understood from the fact that the initial distribution of the matter corresponds to atoms condensed at the maxima of the potential (i.e., positions of unstable equilibrium). Notice that instability develops very quickly [already at time $t = 15$, which is due to the large positive inverse effective mass; see Fig. 3(b)], out of which two-component bright soliton states emerge, as clearly seen at time $t = 40$. The bright soliton consists of two coupled solitons (one for each component), one bigger than the other. In Figs. 5(a) and 5(b), the time evolution of the unstable sn-cn solutions with different amplitude ratio of the sn and cn components is shown. In both cases the two components are excited at the gap edges corresponding to effective masses having different signs and thus they cor-

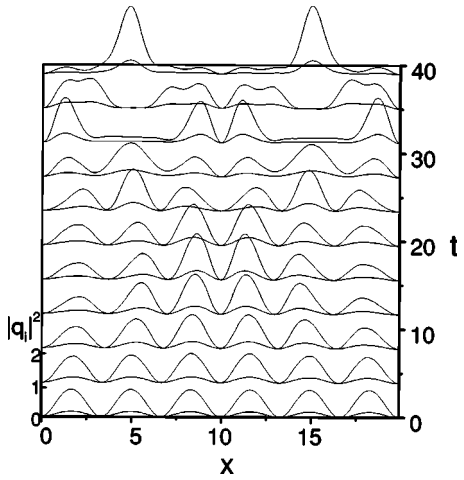

FIG. 4. Prospective view of the time evolution of the unstable sn-sn solution (notice that both components of the solution are depicted at each time). The initial amplitudes are taken as $\gamma_1 = 0.414\,039$, $\gamma_2 = 0.925\,820$. Parameters are fixed as in Fig. 1, except for $k^2 = 0.2$. The modulational initial profile is taken as in Fig. 2. Notice the emergence of coupled soliton components out of the instability.

respond to the second case considered above, where Eq. (5.11) is the condition for the wave stability. In Fig. 5(a) the stable cn component is larger than the unstable sn one, while in Fig. 5(b) we have the opposite. We see that, although in both cases instability develops, the solution with larger stable component is more stable and less effective in creating localized states than the other. This "induced" stabilization is in qualitative agreement with the prediction of the above analysis (a detailed quantitative study of the instability of all possible mixing of stable and unstable components requires more investigations and it will be reported elsewhere).

It is interesting to investigate also solutions involving dn components since these, in contrast with sn and cn components, have nonzero spatial average, i.e., they are periodic waves on top of a constant background. In Fig. 6 we depict the time evolution of a dn-dn solution from which we see that it is modulationally unstable, leading to the formation of bright solitons of the same type observed for the sn-sn case. Similar time evolutions are also reported in Figs. 7 and 8 for the cases sn-dn and cn-dn. Also in this case we observe that the mixing with the unstable sn component is more effective than the one with the stable cn component in creating localized excitations of soliton type (the three bright solitons formed in Fig. 7 at time $t \approx 10$ remain equally spaced and well localized also for longer times). By increasing the cn component of the cn-dn solution of Fig. 8, we also find that the time evolution becomes more stable, as discussed for the sn-cn case. A more detailed numerical analysis is, however, required to characterize the dependence of the modulational instability on the many system parameters.

Before closing this section it is worth discussing the physical implications of the above results. First we remark that in the absence of an optical lattice (periodic potential) a homogeneous condensate with attractive (repulsive) interactions, negative (positive) b_j in our case, is unstable (stable) with respect to long wavelength perturbations. In this section

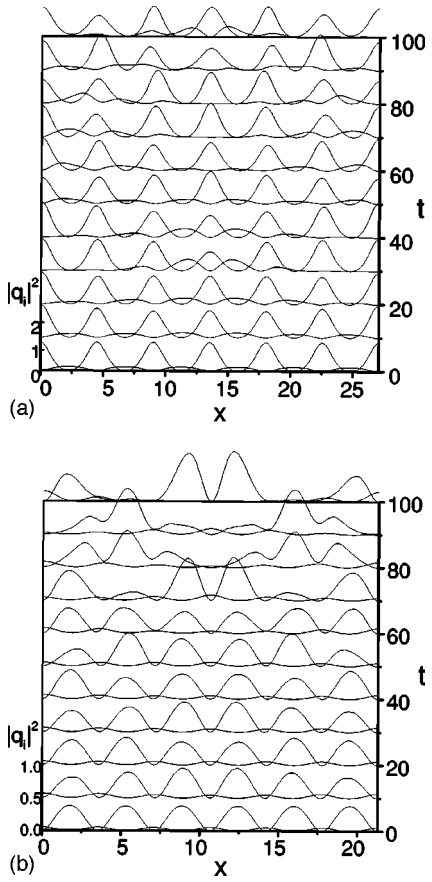

FIG. 5. (a) Same as in Fig. 4 but for the unstable sn-cn solution. The initial amplitudes are taken as $\gamma_1 = 0.411\,113$ and $\gamma_2 = 1.0877$. Parameters are fixed as in Fig. 1 except for $b_0 = -0.65$. Notice that the cn component is larger and more stable. (b). Same as in Fig. 4 but for the unstable cn-sn solution. The initial amplitudes are taken as $\gamma_1 = 0.237\,356$, and $\gamma_2 = 0.627\,986$. Parameters are fixed as in Fig. 1 except for $k^2 = 0.4$ and $b_0 = -0.65$. Notice that the unstable sn component dominates and soliton generation is more effective.

we have shown that, similarly to the one-component case (see [3]), the presence of a periodic potential dramatically changes the situation, allowing existence of modulationally stable and unstable Bloch waves independently of the type of the interaction. Also, in complete analogy with the one-component case, instabilities of Bloch waves can be used for the sake of generation of solitary pulses (more precisely, coupled spatially localized states of both components). In this regard we remark that localized excitations obtained from trivial phase solutions are not stationary in time but have complicated dynamics, as is natural for waves produced from modulational instability. A simple way to stabilize them in time, however, is to increase the strength of the periodic potential when localized excitations are formed. This has the effect of enhancing the confinement, by reducing the atomic tunneling between potential wells, with the result of dynamical stabilization (stationary states are produced after some transient). In Fig. 9 we show an example of this stabilization for the case of the sn-sn solution in Fig. 4. In particular, panel (a) of Fig. 9 shows the early stages of the time evolution while panel (b) shows the dynamics of the stable multi-

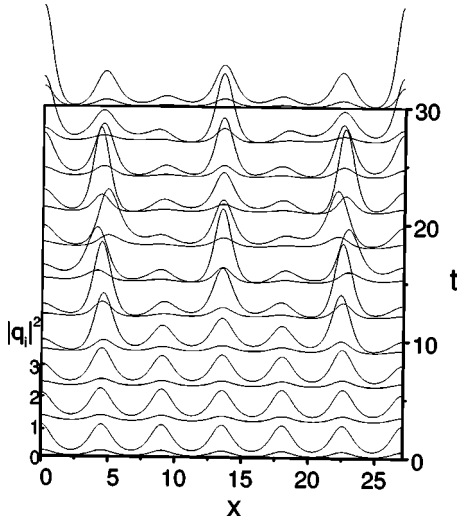

FIG. 6. Same as in Fig. 4 but for the unstable dn-dn solution. Initial amplitudes are $\gamma_1 = -0.462\,91$ and $\gamma_2 = 1.035\,099$. Other parameters are fixed as in Fig. 1.

component soliton which is formed at later stages. For this case, the strength of the potential was increased at time $t = 15$ by a factor of 6 with respect to its initial value. Outflow boundary conditions were used to eliminate the excess matter and to isolate the single two-component soliton. Notice that by increasing the potential strength just after the modulational instability has developed, two (two-component) solitons have been trapped in the middle of the line [see Fig. 9(a)]. This solution, however, is unstable and after a long transient it evolves into a stable single multicomponent soliton oscillating in the potential well [see Fig. 9(b)], remaining stable for the rest of the time (notice that the two components move in phase). Two-hump–single-hump transitions were also observed in the single component NLS equation with periodic potential [21,22] where the analogy with intrinsic localized modes of discrete lattices was emphasized. The above stabilization technique was also shown to be effective for multidimensional solitons [19].

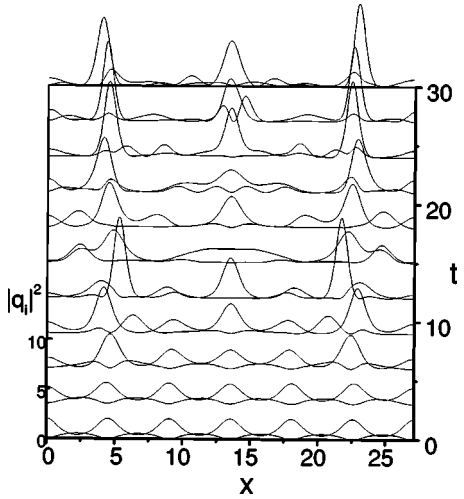

FIG. 7. Same as in Fig. 4 but for the sn-dn solution. Initial amplitudes are $\gamma_1 = 0.738\,55$ and $\gamma_2 = 1.430\,19$. Other parameters are fixed as in Fig. 1 except for $b_0 = -0.7$.

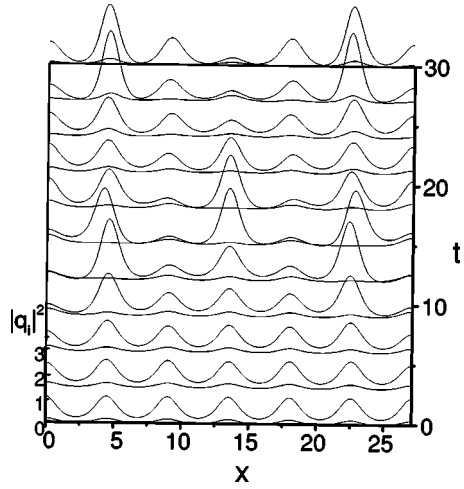

FIG. 8. Same as in Fig. 4 but for the cn-dn solution. Initial amplitudes are $\gamma_1 = 0.414\,04$ and $\gamma_2 = 1.035\,10$. Other parameters are fixed as in Fig. 1.

VI. DISCUSSION

In this section we briefly discuss the Hamiltonian properties of the n-component NLS-type equation with external potential, whose strength can be different for each component [11]:

$$i\frac{\partial \psi_j}{\partial t} = -\frac{1}{2\mu_j}\frac{\partial^2 \psi_j}{\partial x^2} + V_j(x)\psi_j + \sum_{p=1}^{n} a_{jp}|\psi_p|^2\psi_j, \qquad (6.1)$$

$$V_j(x) = -V_{0j}\mathrm{sn}^2(\alpha x, k), \quad j = 1,\ldots,n. \qquad (6.2)$$

Such NLS-type equations with symmetric interacting matrices $a_{jp} = a_{pj}$ are natural generalizations of Eqs. (3.2) and (3.3). The Hamiltonian of Eq. (6.1) is

$$H = \int dx \left[\sum_{j=1}^{n} \frac{1}{2\mu_j}\left|\frac{\partial \psi_j}{\partial x}\right|^2 + \frac{1}{2}\sum_{j,p=1}^{n} a_{jp}|\psi_j|^2|\psi_p|^2 + \sum_{j=1}^{n} V_j(x)|\psi_j|^2 \right], \qquad (6.3)$$

where the integration goes over one period $0 \leqslant x \leqslant L$.

It is pointed out in Ref. [11] that nontrivial as well as trivial phase solutions exist for generic choices of the parameters only provided the interaction matrix a is invertible. The $n = 2$ cases with degenerate a may exist for special choices of the parameters; see Secs. III and IV.

Here we remark that for some *Ansätze* the n-component NLS equation reduces to an effective one-component NLS-type equation. Indeed, let us choose

$$\psi_j(x) = n_j(x,t)\psi(x,t), \quad n_j(x,t) = e^{-i\omega_j t + i\Theta_j(x)}\sqrt{N_j}, \qquad (6.4)$$

where $N_j > 0$ and $\Theta_j(x)$ appears only in the nontrivial phase case and is determined by

$$\frac{d\Theta_j}{dx} = \frac{\mathcal{C}_j}{N_j|\psi(x)|^2}. \qquad (6.5)$$

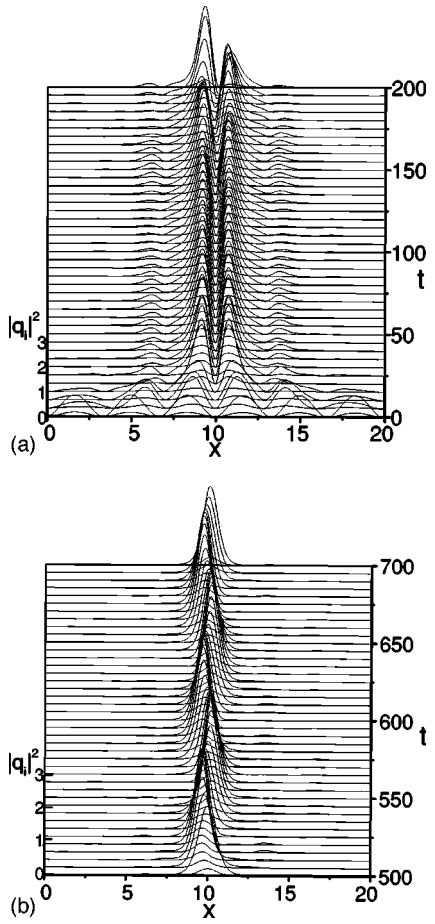

FIG. 9. Time evolution of a two-component soliton resulting from the modulational instability of the sn-sn solution. Parameters are the same as in Fig. 4. (a) Early stages of the stabilization process. (b) The two-component soliton oscillating inside the potential well at later stages of the time evolution. The soliton dynamics has been stabilized by increasing the strength of the periodic potential by a factor of 6 with respect to the initial value at the early stages ($t=15$) of the instability process. Outflow boundary conditions have been used to eliminate the excess matter.

Inserting Eq. (6.4) into the Hamiltonian we easily get the following reduced Hamiltonian $H=H_0+H_{\rm red}$, where:

$$H_{\rm red}=\int dx\left[\frac{M_0}{2}\left|\frac{\partial\psi}{\partial x}\right|^2+\frac{M_{-1}}{2|\psi|^2}+V(x)|\psi|^2+\frac{W_0}{2}|\psi|^4\right],$$

$$M_0=\sum_{j=1}^{n}\frac{N_j}{\mu_j},\quad M_{-1}=\sum_{j=1}^{n}\frac{C_j^2}{N_j\mu_j},$$

$$V(x)=v_0\,\mathrm{sn}^2(\alpha x,k),\quad W_0=\sum_{j,p=1}^{n}a_{jp}N_jN_p,$$

$$v_0=\sum_{j=1}^{n}V_{0j}N_j,\quad H_0=\sum_{j=1}^{n}\frac{C_j}{\mu_j}\arg\psi(x,t)\Big|_{x=0}^{L},\qquad(6.6)$$

which describes the dynamics of the effective field $\psi(x,t)$. The result for the trivial phase solution case is obtained with $C_j=0$ and leads to $H_{\rm red}$ with $M_{-1}=0$. This means that the systems of n equations with the *Ansatz* (6.4) reduce to just one equation for $\psi(x,k)$; the remaining $n-1$ equations follow as a consequence of the first one and the set of constraints on the coefficients $a_{jl},N_j,\mu_j,\omega_j$. The same argument holds true also for three of our solutions, cases 4, 5, and 6. In particular the solutions cn-cn, sn-sn, and dn-dn are effectively one-component ones. The class of solutions that describe the multicomponent effects should be analyzed by using *Ansätze* more general than (6.4). The stability properties of these solutions do not seem to be trivial consequences of the theorems proved in [11] and deserve additional studies. It is also worth remarking that our numerical results are complementary to the ones in Ref. [11] due to the facts that (i) our interaction matrices a are chosen to be negative definite, while in [11] a is positive definite; (ii) our external potential has sign opposite to the one in [11]. These two differences account for the different stability properties of otherwise seemingly equivalent solutions, e.g., cn-cn and dn-dn.

Before closing this section, we shall briefly discuss possible experimental realizations of the described phenomena. To this regard, we remark that for condensates with repulsive interactions one could achieve desired initial states by adiabatic switching on the lattice potential, allowing atoms to acquire a stable distribution, which subsequently can be made unstable by means of abrupt change of the lattice parameters or by accelerating the lattice until the state approaches the edge of the Brillouin zone, where modulational instability develops. In the case of attractive interactions, to avoid the phenomenon of collapse present in the multidimensional case, one should prepare the apparatus so as to conform to the criterion of validity of the 1D approximation. In this case, the respective initial conditions could be created by switching the sign of the interactions by means of a Feshbach resonance [23]. Thus, one could start from a two-component BEC with negligibly small scattering lengths (i.e., a gas of almost noninteracting atoms), first loaded in an optical lattice in a stable uniform atomic configuration and subsequently exposed to an external magnetic field, allowing effective control of the signs and magnitudes of the scattering lengths via the Feshbach resonance. In this situation the two-component BEC should either remain stable or develop instabilities of the type described above, depending on the sign of the scattering lengths. We hope these results will be of interest to experimentalists working on mixtures of Bose-Einstein condensates.

VII. CONCLUSIONS

In conclusion, we have considered the two-component CNLS equation with an elliptic potential as a model for trapped, quasi-one-dimensional two-component BEC's. Classes of elliptic solutions have been analyzed in detail. In particular we considered intrinsic two-component solutions, i.e., ones with nonproportional amplitudes. The role played by these solutions as initial states from which localized mat-

ter waves (solitons) can be generated through the modulational instability mechanism has been shown.

Further perspectives of finding stable periodic solutions to the n-component case are outlined in [16]. For $n=2$ finite-gap solutions of Manakov system given in terms of multidimensional θ functions are derived in [24,25]; reduction of finite-gap solutions to elliptic functions is presented in [13]. Interesting classes of periodic solutions can also be obtained as the result of reduction of the Manakov system to a completely integrable two-particle system interacting with fourth order potential [15,26].

Recently, we became aware of Ref. [27] which gives extra evidence for the correctness of our results and their agreement with the ones in [28].

ACKNOWLEDGMENTS

We thank Dr. B. Baizakov for useful discussion and for his assistance with the numerical parts. V.V.K. acknowledges Professor B. Deconinck for discussing results in Ref. [11] prior to their publication. V.S.G. and V.Z.E. wish to thank the Department of Physics "E. R. Caianiello" for the hospitality received, and the University of Salerno for providing an eight-month research grant during which most of this work was done. V.V.K. acknowledges support from the European Grant COSYC No. HPRN-CT-2000-00158. M.S. acknowledges partial financial support from the MIUR, through the interuniversity project PRIN-2003, and from the INFN (Istituto Nazionale di Fisica Nucleare) Sezione di Salerno.

[1] F. Dalfovo, S. Giorgini, L. P. Pitaevskii, and S. Stringari, Rev. Mod. Phys. **71**, 463 (1999).
[2] V. M. Pérez-García, H. Michinel, and H. Herrero. Phys. Rev. A **57**, 3837 (1998); H. Michinel, V. M. Pérez-García, and R. de la Fuente, *ibid.* **60**, 1513 (1999); L. D. Carr, M. A. Leung, and W. P. Reinhardt, J. Phys. B **33**, 3983 (2000).
[3] V. V. Konotop and M. Salerno, Phys. Rev. A **65**, 021602(R) (2002).
[4] F. Barra, P. Gaspard, and S. Rice, Phys. Rev. E **61**, 5852 (2000).
[5] J. C. Bronski, L. D. Carr, B. Deconinck, and J. N. Kutz, Phys. Rev. Lett. **86**, 1402 (2001).
[6] L. D. Carr, J. N. Kutz, and W. P. Reinhardt, Phys. Rev. E **63**, 066604 (2001).
[7] J. C. Bronski, L. D. Carr, B. Deconinck, J. N. Kutz, and K. Promislow, Phys. Rev. E **63**, 036612 (2001).
[8] D. M. Stamper-Kurn, M. R. Andrews, A. P. Chikkatur, S. Inouye, H.-J. Meisner, J. Stenger, and W. Ketterle, Phys. Rev. Lett. **80**, 2027 (1998); D. S. Hall, M. R. Matthews, J. R. Ensher, C. E. Wieman, and E. A. Cornell, *ibid.* **81**, 1539 (1998)
[9] M. Modugno, F. Dalfovo, C. Fort, P. Maddaloni, and F. Minardi, Phys. Rev. A **62**, 063607 (2000).
[10] T. Busch and J. R. Anglin, Phys. Rev. Lett. **87**, 010401 (2001).
[11] B. Deconinck, J. N. Kutz, M. S. Patterson, and B. W. Warner. J. Phys. A **36**, 5431 (2003).
[12] S. V. Manakov, Zh. Eksp. Teor. Fiz. **67**, 543 (1974) [Sov. Phys. JETP **38**, 248 (1974)].
[13] E. D. Belokolos, A. I. Bobenko, V. Z. Enolskii, A. R. Its, and V. B. Matveev, *Algebro-Geometric Approach to Nonlinear Integrable Equations* (Springer, Berlin, 1994).
[14] A. V. Porubov and D. F. Parker, Wave Motion **29**, 97 (1999).
[15] P. L. Christiansen, J. C. Eilbeck, V. Z. Enolskii, and N. A. Kostov, Proc. R. Soc. London, Ser. A **456**, 2263 (2000).
[16] J. C. Eilbeck, V. Z. Enolskii, and N. A. Kostov. J. Math. Phys. **41**, 8236 (2000).
[17] P. Maddaloni, M. Modugno, C. Fort, F. Minardi, and M. Inguscio, Phys. Rev. Lett. **85**, 2413 (2000).
[18] G. P. Agrawal, *Nonlinear Fiber Optics*, 2nd ed. (Academic, San Diego, 1995).
[19] B. B. Baizakov, V. V. Konotop, and M. Salerno, J. Phys. B **35**, 5105 (2002).
[20] *Handbook of Mathematical Functions*, edited by M. Abramowitz and I. A. Stegun (Dover, New York, 1965).
[21] E. Alfimov, V. V. Konotop, and M. Salerno, Europhys. Lett. **58**, 7 (2002).
[22] Mario Salerno, e-print. cond-mat/0311630.
[23] S. Inouye *et al.*, Nature (London) **392**, 151 (1998); E. A. Donley *et al.*, *ibid.* **412**, 295 (2001).
[24] M. R. Adams, J. Harnad, and J. Hurtubise, Commun. Math. Phys. **155**, 385 (1993).
[25] J. N. Elgin, V. Z. Enolskii, and A. R. Its, Physica D (to be published).
[26] P. L. Christiansen, J. C. Eilbeck, V. Z. Enolskii, and N. A. Kostov, Proc. R. Soc. London, Ser. A **451**, 685 (1995).
[27] E. A. Ostrovskaya and Y. S. Kivshar, Phys. Rev. Lett. **92**, 180405 (2004).
[28] A. A. Sukhorukov and Y. S. Kivshar, Phys. Rev. Lett. **91**, 113902 (2003).